AD-A 083 866

TECHNICAL REPORT ARBRL-TR-02221

DYNAMICS OF A LIQUID-FILLED GYROSCOPE: UPDATE OF THEORY AND EXPERIMENT

Richard D. Whiting
Nathan Gerber

March 1980

US ARMY ARMAMENT RESEARCH AND DEVELOPMENT COMMAND
BALLISTIC RESEARCH LABORATORY
ABERDEEN PROVING GROUND, MARYLAND

Approved for public release; distribution unlimited.

REPORT DOCUMENTATION PAGE

READ INSTRUCTIONS BEFORE COMPLETING FORM

1. REPORT NUMBER TECHNICAL REPORT ARBRL-TR-02221	2. GOVT ACCESSION NO.	3. RECIPIENT'S CATALOG NUMBER
4. TITLE (and Subtitle) DYNAMICS OF A LIQUID-FILLED GYROSCOPE: UPDATE OF THEORY AND EXPERIMENT		5. TYPE OF REPORT & PERIOD COVERED Final 6. PERFORMING ORG. REPORT NUMBER
7. AUTHOR(s) Richard D. Whiting Nathan Gerber		8. CONTRACT OR GRANT NUMBER(s)
9. PERFORMING ORGANIZATION NAME AND ADDRESS U.S. Army Ballistic Research Laboratory (ATTN: DRDAR-BLL) Aberdeen Proving Ground, Maryland 21005		10. PROGRAM ELEMENT, PROJECT, TASK AREA & WORK UNIT NUMBERS RDT&E 1L161102AH43
11. CONTROLLING OFFICE NAME AND ADDRESS U.S. Army Armament Research & Development Command U.S. Army Ballistic Research Laboratory (ATTN: DRDAR-BL) Aberdeen Proving Ground, MD 21005		12. REPORT DATE MARCH 1980 13. NUMBER OF PAGES 51
14. MONITORING AGENCY NAME & ADDRESS(if different from Controlling Office)		15. SECURITY CLASS. (of this report) Unclassified 15a. DECLASSIFICATION/DOWNGRADING SCHEDULE

16. DISTRIBUTION STATEMENT (of this Report)

Approved for public release; distribution unlimited.

17. DISTRIBUTION STATEMENT (of the abstract entered in Block 20, if different from Report)

18. SUPPLEMENTARY NOTES

19. KEY WORDS (Continue on reverse side if necessary and identify by block number)

Eigenfrequencies
Yaw Growth Rate
Liquid-Filled Shell
Gyroscope Experiments
Solid-Body Rotation
Coning Frequencies
Stewartson-Wedemeyer Theory
Liquid-Filled Gyroscopes

20. ABSTRACT (Continue on reverse side if necessary and identify by block number) (lcb)

New comparisons are made between the theory of Stewartson, as modified by Wedemeyer, and existing experimental measurements of the motion of liquid-filled gyroscopes. Errors in previous comparisons are pointed out and corrected, as are some errors in several published presentations of the theory. Because some key parameters were not recorded during the experiments, complete comparisons of theoretical predictions with observed behavior cannot be made. The limited comparisons which can be made show that predicted and measured (Continued)

20. ABSTRACT (Continued):

frequencies of greatest instability of the motion agree to within the experimental error; the growth rates at those frequencies agree to within 10% for Reynolds number > 10^4, and to within 25% for lower Reynolds number.

TABLE OF CONTENTS

LIST OF FIGURES

LIST OF FIGURES (Continued)

I. INTRODUCTION

A. Background

In 1959 K. Stewartson[1] published a theory on the motion of a top containing a rigidly-spinning inviscid liquid in a cylindrical cavity; this theory is equally applicable to shell and gyroscopes. In conjunction with this theory the gyroscope provides an excellent laboratory tool for studying the yawing motion of a spinning liquid-filled shell.

Stewartson predicted the existence of instabilities in the motion of the top due to resonances between oscillations of the liquid and nutation of the top. Ward[2] experimentally confirmed the presence of two of the predicted instabilities in a gyroscope, though his results differed in detail from the prediction. Experiments conducted at the BRL by Karpov[3,4] with liquid-filled shell and with liquid-filled gyroscopes also confirmed the presence of instabilities, but showed a strong dependence of the growth rate of the instabilities on the viscosity of the liquid. Wedemeyer[5,6] developed a theory of viscous corrections to Stewartson's theory which predicted viscous effects of the nature of those found by Karpov; his comparison of the theory with Karpov's experiments was flawed, as discussed below. Frasier and

---

1. *K. Stewartson, "On the Stability of a Spinning Top Containing Liquid," Journal of Fluid Mechanics, Vol. 5, Part 4, September 1959, pp. 577-592.*

2. *G. N. Ward, Appendix to Reference 1.*

3. *B. G. Karpov, "Dynamics of a Liquid-Filled Shell: Resonance and the Effects of Viscosity," BRL Report No. 1279, U.S. Army Ballistic Research Laboratory, Aberdeen Proving Ground, Maryland, May 1965. AD 468654.*

4. *B. G. Karpov, "Liquid Filled Gyroscope: The Effect of Reynolds Number on Resonance," BRL Report No. 1302, U.S. Army Ballistic Research Laboratory, Aberdeen Proving Ground, Maryland, October 1965. AD 479430.*

5. *E. H. Wedemeyer, "Dynamics of Liquid-Filled Shell: Theory of Viscous Corrections to Stewartson's Stability Problem," BRL Report No. 1287, U.S. Army Ballistic Research Laboratory, Aberdeen Proving Ground, Maryland, June 1965. AD 472474.*

6. *E. H. Wedemeyer, "Viscous Corrections to Stewartson's Stability Criterion," BRL Report No. 1325, U.S. Army Ballistic Research Laboratory, Aberdeen Proving Ground, Maryland, June 1966. AD 489687.*

Scott[7] developed a theory analogous to Stewartson's for a gyroscope with a solid rod concentric with the cylindrical cavity. They predicted that the presence of the rod primarily would change the natural frequencies of the liquid, the motion itself remaining similar to that without the rod. Frasier[8] applied Wedemeyer's theory of viscous corrections to this case and performed gyroscope experiments to check the theory.

Karpov and Wedemeyer used the works mentioned above, plus others, as the foundation for Ref. 9, the handbook for liquid-filled projectile design. Ref. 9 presents theoretical and experimental results as well as operational formulas intended for use by designers in assessing the stability of liquid-filled projectiles. Since the preparation of the handbook, D'Amico[10], Scott and D'Amico[11], and Kitchens (unpublished) have performed experiments in which growth rates of the unstable motions of liquid-filled gyroscopes were measured. The object of most of these experiments was to observe changes in growth rate with large amplitude of the motion, and no comparison has been reported between the results of these experiments and the linear, small amplitude theory of Stewartson-Wedemeyer, though such comparison is possible.

B. Purpose of This Report

Wedemeyer's theory of viscous corrections for solid-body rotation consists of two distinct parts: (1) a theory of viscous effects on oscillations of the liquid, and (2) a theory of the response of the gyroscope to the oscillations. At the time Karpov[4] was reporting his final experiments, only the second part of the theory had been developed--Wedemeyer could predict the motion of the gyroscope given the oscillations of the liquid, but could not accurately predict the frequencies and damping factors of these oscillations.

7. *J. T. Frasier and W. E. Scott, "Dynamics of a Liquid-Filled Shell: Cylindrical Cavity With a Central Rod," BRL Report No. 1391, U.S. Army Ballistic Research Laboratory, Aberdeen Proving Ground, Maryland, October 1968. AD 667365.*

8. *J. T. Frasier, "Dynamics of a Liquid-Filled Shell: Viscous Effects in a Cylindrical Cavity With a Central Rod," BRL Memorandum Report No. 1959, U.S. Army Ballistic Research Laboratory, Aberdeen Proving Ground, Maryland, January 1969. AD 684344.*

9. *Engineering Design Handbook, Liquid-Filled Projectile Design, AMC Pamphlet No. 706-165, U.S. Army Materiel Development and Readiness Command, Washington, D. C., April 1969. AD 853719.*

10. *W. P. D'Amico, "Inertial Mode Corrections for the Large Amplitude Motion of a Liquid-Filled Gyroscope," PhD Thesis, University of Delaware, Newark, Delaware, June 1977.*

11. *W. E. Scott and W. P. D'Amico, "Amplitude-Dependent Behavior of a Liquid Filled Gyroscope," J. Fluid Mech., Vol. 60, Part 4, October 1973, pp. 751-758.*

Karpov used his measurements of the motion of the gyroscope and the second part of the theory to find the liquid frequencies and damping factors at resonance, as explained in Section 5 of Ref. 4. Fig. 3 of this reference shows the resulting damping factors. Karpov used these values and the second part of the theory (Eq. (5) in Ref. 4) to compute the growth rate of the motion of the gyroscope away from resonance. This calculated growth rate is shown by the solid curves in Figs. 4 and 5 of Ref. 4; the circles in those figures are data. Because it was necessary to use the measured resonance growth rate itself in predicting other growth rates, the theoretical results could only predict the shape of the growth rate (vs. an appropriate parameter) curve in the neighborhood of resonance. There was no check of the magnitude of the growth rate at any frequency.

Fig. 1 of Ref. 6 presents the same information as Figs. 4 and 5 of Ref. 4. Thus, despite the statements at the bottom of p. 22 of Ref. 6, these figures present only a very limited check of theory with experiment. These same diagrams are presented as Fig. 6-2 of Ref. 9; in the text preceeding the figure (Section 6-4) a succinct explanation is given of the way in which the solid curves were actually computed. Note that in this explanation, the relation*

$$[|D|/(\sigma L)]^{\frac{1}{2}} = 1.6 \times 10^{-3}$$

is given as descriptive of the cylinder. The meaning of this quantity will be explained later; what is of significance here is that for the reported experiment, it was <u>not</u> constant, varying by more than a factor of two over the experimental range. Thus, the first part of Wedemeyer's theory has not been checked at all against Karpov's data, and the second part has not been checked consistently.

Frasier modified the theory for the rodded case[8] by Wedemeyer's viscous correction technique. The comparison between the modified theory and experimental data is flawed, however, because the theory was not correctly evaluated. A discussion of the nature of the error is deferred until Section III.

The experiments conducted after the release of the liquid-filled projectile handbook, Ref. 9, have not been used to check Wedemeyer's theory, in part because they were intended for other purposes. Thus, because of the difficulties with Karpov's and Frasier's comparisons, the situation exists that the theory, which forms a substantial part of the handbook, has never been adequately checked against experimental data, though data are available.

The primary purpose of this report is to present a comparison of the theory with all of the data from gyroscope experiments conducted

* *Definitions are given in List of Symbols section, p. 33.*

at BRL, so that a proper assessment of its validity can be made. In addition, some significant misstatements and errors in equations in Ref. 9 are pointed out and corrected.

II. THEORY

A. Equations of Motion of the Gyroscope

A brief sketch of the theory is given here; the reader is referred to Refs. 1, 6, 7, and 9 for details. The purpose here is to show where the theory is susceptible to experimental confirmation.

The gyroscope, shown schematically in Fig. 1, consists of (1) a rotor spinning around its symmetry axis at angular speed Ω, and (2) mounts which allow the rotor (z') axis to yaw about a fixed line (z-axis) through the "point of support" (the point defined by the intersection of lines drawn through the gimbal pivots). Let the (x,y,z) coordinate system be an inertial system with the x-axis passing through the outer gimbal pivots and the z-axis parallel to gravity. Let the non-rotating (x', y', z') coordinate system be attached to the inner gimbal mount in such a way that when the z and z' axes coincide, the x and x' and y and y' axes also coincide.

Fig. 2 shows coordinates (the x' and y' axes being omitted for the sake of clarity). The z'-axis is coning about the z-axis at a small yaw angle, $\alpha(t)$, where $\alpha << 1$. The yawing motion of the gyroscope is described by the component angles θ_x and θ_y of the projection of the end point of a unit vector in the z'-direction upon the x-y plane, as shown in the figure. We combine these components in the complex yaw $\theta = \theta_x + i\,\theta_y$.

The liquid is confined in a cylindrical cavity whose symmetry axis coincides with that of the rotor; the radius of the cavity is a, and the length is 2c. For a partially-filled cavity, the fraction of fill is $1 - b^2/a^2$, where b is the inner radius of a concentric annulus with volume equal to that of the liquid. In the case of a rodded cylinder, the air core is replaced by a rigid rod of radius d.

There are two torques acting on the gyroscope, the first caused by gravity acting on the mass of the gyroscope, and the second caused by the liquid. Assuming small θ, we denote the first moment by $M_o\theta$ and the second moment by $\overset{*}{\Gamma}\theta$, where M_o is a real constant (= 0 when the pivot point and center of mass coincide) and $\overset{*}{\Gamma}$ $(\theta, d\theta/dt)$ is a complex function. The equation of motion of the gyroscope when $|\theta|$ is small (see, e.g., pp. 2-14 and 3-11 in Ref. 9) is

$$T\, d^2\theta/dt^2 - iL\Omega\, d\theta/dt - M_o\theta = -\overset{*}{\Gamma}\,(\theta,\, d\theta/dt)\,\theta \quad , \tag{1}$$

where L is the axial moment of inertia of the gyroscope, and T is the transverse moment of inertia about the pivot point. The moments of inertia about the x' - and y' -axes must be approximately equal here; see p. 2-13 of Ref. 9 for discussion.

Because of the dependence of $\overset{*}{\Gamma}$ on θ, Eq. (1) is non-linear; the solution to an initial value problem cannot in general be constructed by linear combination of independent solutions.*

B. Exponential Solutions

For certain values of the complex constant τ, possible solutions of Eq. (1) are

$$\theta = \theta_o \exp\,(i\,\tau\,\Omega\,t) \quad . \tag{2}$$

These solutions constitute the bases of the Stewartson-Wedemeyer analyses, particularly in regard to establishing criteria for stable motion. The permissible values of τ are found by substituting Eq. (2) into Eq. (1), which gives

$$T\,\tau^2 - L\,\tau + (M_o/\Omega^2) = \Gamma\,(\tau)/\Omega^2 \quad . \tag{3}$$

Once the liquid moment function, $\Gamma\,(\tau)$, is provided, Eq. (3) is solved for τ.

Let $\tau = \tau_R + i\,\tau_I$.** Eq. (2) then represents an angular motion, here called coning motion, of constant frequency, $\tau_R\Omega$, which decays with time at the rate $\tau_I\Omega$ if τ_I is positive, but grows in amplitude and becomes unstable if τ_I is negative. The quantity $-\tau_I$ is called the "yaw growth rate", and its measurement is the primary objective of gyroscope experiments.

---

* *In this regard the statement following Eq. (4-17) in Ref. 9 is misleading.*

** *In the original inviscid perturbation theory of Stewartson, τ is real for certain regions in parameter space; see the un-numbered equation preceeding Eq. (5.12) in Ref. 1.*

The forcing term on the right-hand side of Eq. (1) is (1) zero if the gyroscope is empty, and (2) negligible if τ_R is <u>not</u> near any natural frequency, τ_{oo}, of free oscillation of the liquid (see bottom p. 10 of Ref. 6), i.e., away from resonance. For either of these conditions, Eq. (3) has two real solutions, denoted by τ_n and τ_p (nutational and precessional frequencies, respectively, of the gyroscope):

$$\tau_n = [L/(2T)]\ [1 + (1 - \beta)^{1/2}] \tag{4}$$

$$\tau_p = [L/(2T)]\ [1 - (1 - \beta)^{1/2}]$$

where

$$\beta = 4\ M_o\ T/(L\Omega)^2 \quad . \tag{5}$$

In these situations, $\theta(t)$ is a linear combination of $\exp(i\ \tau_n\ \Omega t)$ and $\exp(i\ \tau_p\ \Omega\ t)$.

The basis for the prediction of yaw growth rate is the premise that near resonance the motion of the gyroscope with liquid is dominated, over a significant time interval, by a single mode of the form

$$\theta = \theta_o \exp(i\ \tau_R\ \Omega\ t)\ \exp(-\ \tau_I\ \Omega\ t) \quad , \tag{6}$$

where τ_I is negative. This premise is supported by experimental evidence and the conclusions of Stewartson-Wedemeyer theories. Then the amplitude of the yaw should behave as

$$\ln\ (\text{modulus}\ [\theta_{meas}]) \cong \text{const} - \tau_I\ \Omega\ t \quad , \tag{6a}$$

which represents a straight line whose slope provides τ_I.

C. <u>Evaluation of the Liquid Moment</u>

Determination of the moment exerted by the liquid on the gyroscope requires solving the appropriate equations of motion for the liquid, subject to boundary conditions determined by the position and motion of the rotor. The solution to these equations yield pressure; integration of the pressure, with the appropriate moment arm,

over the inner surface of the rotor would give the liquid moment.* To the authors' knowledge no one has actually carried out this integration. The integration can be avoided in the region of resonance ($\tau_R \approx \tau_{oo}$) by employing an approximation of Stewartson[1].

C.1. Inviscid Theory: Approximation Near Resonance.

The moment exerted by an inviscid liquid is very small unless the coning frequency τ is near one of the liquid natural frequencies τ_o. If τ is near τ_o, i.e., $|\tau_R - \tau_o|$ and $|\tau_I|$ <<1, then Γ can be approximated in Eq. (3) by

$$\Gamma\ (\tau) \simeq \Omega^2\ D\ (\tau_o)\ /\ (\tau - \tau_o) \quad , \tag{7}$$

where D is the residue of a Laurent series expansion about $\tau = \tau_o$. It is convenient to define a non-dimensional quantity R:

$$R^2 = -\ D\ (\tau_o)\ c\ /\ (\rho\ a^6) \quad . \tag{8}$$

The eigenfrequencies τ_o and the residues R depend only on c/a, b/a, and the azimuthal, axial, and radial wave numbers of the liquid wave: m, j, and n. Only singly-periodic waves (m = 1) contribute to the moment, and only they are considered hereafter.

Tables of τ_o and 2R vs c/[(2j + 1) a] and b^2/a^2 are presented in Ref. 1** for cylinders without a central rod, and in Ref. 7 (d replacing b***) for cylinders with a central rod. Expanded versions of both tables are presented in Ref. 9.

C.2. Viscous Correction for Large Reynolds Number

For quantitative purposes the effect of viscosity cannot be neglected in the prediction of eigenfrequencies, and consequently, of yaw growth rates. Wedemeyer[6] demonstrated that for large Reynolds numbers, Re ($\equiv a\Omega^2/\nu$), a viscous correction to the inviscid eigenfrequency can be derived. In the formalism of his treatment, the

---

* *We note that minus signs should appear before the integrals on the right-hand sides of Eqs. (3-31) and (3-30a) in Ref. 9.*

** *In Ref. 1, Tables 1-5, the column labeled "R" should be labeled "2R".*

*** *The "b^2/a^2" labeling on pp. 53-67 of Ref. 7 should be replaced by "d^2/a^2".*

viscous eigenfrequency τ_{ov} ($\equiv \tau_{oo} + i\delta$) is complex, with a viscous damping factor δ; τ_{oo} differs from τ_o. The presence of boundary layers on the cylinder walls effectively changes the cavity dimensions to a-δa, c-δc, and d+δd, where the complex increments δa, δc, and δd are given by*:

$$\delta a/a = (2Re)^{-\frac{1}{2}} (1 + i) (1 - \tau_o)^{-\frac{1}{2}} \tag{9a}$$

$$\delta c/c = \frac{(2Re)^{-\frac{1}{2}}}{2(1-\tau_o)} \frac{a}{c} \left[\frac{(1-i)(3-\tau_o)}{(1+\tau_o)^{\frac{1}{2}}} - \frac{(1+i)(1+\tau_o)}{(3-\tau_o)^{\frac{1}{2}}} \right] \tag{9b}$$

$$\delta d/d = a/d\ (\delta a/a) \quad . \tag{9c}$$

The viscous eigenfrequency is then obtained formally as a first-order correction to τ_o. For a cylinder with no central rod,

$$\tau_{ov} = \tau_o + \left[\frac{c}{a(2j+1)} \frac{\partial \tau_o}{\partial [c/a(2j+1)]} \right] \left[\frac{\delta a}{a} - \frac{\delta c}{c} \right] + \left[\frac{2b^2}{a^2} \frac{\partial \tau_o}{\partial (b^2/a^2)} \right] \frac{\delta a}{a} \tag{10}$$

For a cylinder with a central rod

$$\tau_{ov} = \tau_o + \frac{c}{a(2j+1)} \frac{\partial \tau_o}{\partial (ca^{-1} \{2j+1\}^{-1})} \left[\frac{\delta a}{a} - \frac{\delta c}{c} \right] + \frac{2d^2}{a^2} \frac{\partial \tau_o}{\partial (d^2/a^2)} \left[\frac{\delta a}{a} + \frac{\delta d}{d} \right] \quad . \tag{11}$$

---

* *Wedemeyer denotes the argument in the right-hand side of Eqs. (17) and (19) of Ref. 6 by τ, calling it the "dimensionless frequency of oscillation". Here he is dealing with free oscillations of the liquid, so τ should be set equal to τ_o. In Ref. 9, Eqs. (6-13) and (6-14) also contain the argument τ, but the succeeding statement "with $\tau = \omega/\Omega$, the dimensionless yawing frequency" is incorrect; however, in the example at the top of p. 6-8, τ is properly set equal to τ_o.*

The effect of viscosity on the liquid moment is then approximated in Wedemeyer's theory by replacing τ_o in Eq. (7) by τ_{ov}, leading to the following new approximation to Eq. (3):

$$T\,\tau^2 - L\,\tau + (M_o/\Omega^2) = D\,(\tau_o)\ /\ [\tau - (\tau_{oo} + i\,\delta)] \quad . \tag{12}$$

D. Solutions for τ

Eq. (12) has three complex roots. Because of the approximation, Eq. (7), made in evaluating the liquid moment, only those roots with $\tau_R \approx \tau_{oo}$ are applicable. If $\tau \approx \tau_p$ or $\tau \approx \tau_n$, the left hand side of Eq. (12) can be approximated by a linear form with an error of $0\,(\tau - \tau_p)^2$ or $0\,(\tau - \tau_n)^2$, respectively. Then Eq. (12) becomes a quadratic. When $\tau \approx \tau_p$, the two roots have positive τ_I's; i.e., the coning motion is damped. When $\tau \approx \tau_n$, the solutions are:

$$\tau_R = \tfrac{1}{2}\,(\tau_n + \tau_{oo}) \mp \tfrac{1}{2}\,\mathrm{sgn}\,(\tilde{n})\ [\tfrac{1}{2}\,\{(m^2 + \tilde{n}^2)^{\frac{1}{2}} - m\}]^{\frac{1}{2}} \tag{13}$$

$$\tau_I = \tfrac{1}{2}\,\delta \pm \tfrac{1}{2}\,[\tfrac{1}{2}\,\{(m^2 + \tilde{n}^2)^{\frac{1}{2}} + m\}]^{\frac{1}{2}} \tag{14}$$

where

$$\sigma = (1 - \beta)^{\frac{1}{2}}$$

$$m = -\,[4\,D(\tau_o)\ /\ (\sigma L)] + \delta^2 - (\tau_n - \tau_{oo})^2 \text{ ---assumed} > 0$$

$$\tilde{n} = 2\,\delta\,(\tau_n - \tau_{oo}).$$

The lower signs in Eqs. (13) and (14) yield negative τ_I, and are thus the signs to use to describe unstable motion of the gyroscope.

Eqs. (13) and (14) are presented as Eqs. (6-7) and (6-8) in Ref. 9. In Ref. 9, Eq. (6-7) is incorrect in that the factor "sgn $(\tilde{n})$", appearing in Eq. (13), is missing from the right-hand side. Additionally, Eq. (6-6) and the definition of $n(=-\tilde{n})$ are inconsistent. Appendix A presents a derivation of Eqs. (13) and (14).

E. Review of Assumptions

It is important to carry out experiments under conditions which do not violate the assumptions of the theory with which measurements will

be compared. It is now proper to state or restate some of the important assumptions inherent in the theory:

1. The rotor cavity is a right circular cylinder (no rounded corners).

2. The unperturbed motion of the liquid is solid-body rotation; also the spin rate is large enough so that in a partially-filled cylinder the void forms a cylinder concentric with the rotor cavity.

3. The Reynolds number of the flow, Re ($\equiv a\Omega^2/\nu$), is very large. Viscous effects are thus confined to thin boundary layers.

4. The coning angle of the gyroscope, $|\theta|$, is small, producing a small perturbation in the solid-body rotation of the fluid.

5. The gyroscope motion is given by Eq. (6), and the perturbed liquid motion has the same exponential dependence on time. This implies that there is an interval of time in which the motion of the coupled gyroscope-liquid system is independent of the realistic initial conditions but satisfies the small amplitude restriction.

6. The coning frequency is in the neighborhood of a liquid eigenfrequency.

7. The liquid mass is much smaller than the mass of the gyroscope. This condition furnishes a simplification in the liquid moment determination.

8. The transverse moments of inertia about the x'- and y'-axes are approximately equal to each other.

III. THE EXPERIMENTS

A. Description

The experiments which will be presented here are those of Karpov[4], Frasier[8], D'Amico[10], Scott and D'Amico[11], and Kitchens (unpublished). All of these experiments were performed at BRL using a gyroscope like that described in Ref. 4.

Two points to be noted are that: (1) only one flexural pivot was equipped with a strain gauge, so that only one component of the coning motion was measured; there was no check made of the assumption of circular coning (see Section II-B); (2) the coning motion of the empty gyroscope was observed to be damped. It was assumed that the observed growth rate of the coning motion of the filled gyroscope (τ_{obs}) could be expressed as the sum of the damping rate of the empty gyroscope (τ_{empty}) and the growth rate of a frictionless filled

gyroscope, i.e.

$$\tau_{obs} = \tau_{empty} + \tau_I \quad . \tag{15}$$

This assumption appears reasonable, although it neglects any interactive effect between mechanical friction and presence of fluid. Thus, the experimental values of yaw growth rate recorded in this report are τ_I, corresponding to the theoretical τ_I of Eq. (14), <u>not</u> the directly measured growth rates. Records indicate that a measured value of $\tau_{empty}\ \Omega = 0.017\ s^{-1}$ was used for several of the experiments, so that $\tau_{empty} \simeq 0.324 \times 10^{-4}$ for $\Omega = 523.6$ rad/sec, the value used in the experiments.

The electrical signal from the strain gauge was recorded on an oscillograph. Since the output of the strain gauge was linear with angular displacement of the flexural pivot, the oscillograph record yielded a plot of coning angle versus time. A set of amplitude readings from the oscillograph record was plotted logarithmically against time. These points fell about a straight line (Eq. (6a)), until the amplitude reached, typically, one degree. The <u>observed</u> yaw growth rate was determined as the slope of this line. The frequency τ_R of the coning motion was measured by counting the number of oscillations between two known times on the oscillograph record. The rotational speed of the cylinder was measured with a stroboscope.

At this late date it is difficult to ascertain the errors of past measurements. A study of these experiments yields estimated relative errors of 2% and 3% for τ_R and τ_I, respectively. These are the errors indicated by the error bars in the figures in this section; the apparent scatter in the data seems to be consistent with these estimates. Estimated errors for cylinder dimensions and fluid parameters are as follows:

Aspect Ratio of Cylinder (c/a)	½-1%
b^2/a^2 (or d^2/a^2)	2%
Reynolds Number (Re)	5%
Liquid Density/Axial Moment of Inertia (ρ/L)	1%

Except for the error in aspect ratio, the effects of these errors on computation of τ_I are small. The effect of the error in c/a can be significant, as discussion in Section III-B will demonstrate.

There is a division between Karpov's experiment and the others, in that Karpov used constant values of L and τ_n, varying the fill ratio of the cylinder (hence the liquid eigenfrequency), while the other experiments varied L and τ_n while maintaining constant fill ratio. Karpov made separate measurements of τ_R and τ_I as functions of b^2/a^2. The others made simultaneous measurements of τ_R and τ_I as functions of L and τ_n, though unfortunately they did not measure or record L or τ_n. <u>This latter fact prevents a full comparison of their experimental data with the theory</u>. The nature of the comparison which can be made is indicated in Section III-C. The Reynolds number was varied by using liquids of varying viscosity, keeping the cylinder speed fixed at 523.6 rad/s. This means that there was no check of the effect of gravity in the experiments with the partially-filled cylinder. Details of cylinder dimensions, liquid properties, moments of inertia, etc., and the measured values of τ_R and τ_I are tabulated in Appendix B.

B. The Results of Karpov

Figs. 3 and 4 present τ_R and $-\tau_I$ for the mode n = j = 1 plotted against b^2/a^2 for the two liquids that Karpov used, labeled #1 (Re = 5.2×10^5) and #2 (Re = 5.2×10^3). The experimental values are indicated by circles and diamonds. The theoretical values, solid curves, are obtained from Eqs. (13) and (14). The plots of $-\tau_I$ against b^2/a^2 are analogous to Figs. 4 and 5 in Ref. 4, Fig. 1 in Ref. 6, and Fig. 6-2 in Ref. 9, where the abscissa is the parameter τ_o. The significant difference between these figures and Figs. 3 and 4 is that the latter two contain true theoretical curves, as opposed to semi-empirical curves in the former (discussed in Section I).

The predicted trend of τ_R seems to appear in the data, as does the "jump" at $b^2/a^2 \approx 0.15$ for liquid #1. However, the data are consistently about 3% higher than the theoretical predictions.

For the Re = 5.2×10^5 case, the measured values of τ_I agree with the predicted values to within the estimated error. For the Re = 5.2×10^3 case, the measured peak value of τ_I is about 10% greater than the prediction, and there is an apparent shift of the measured curve to the left of the theoretical curve. A study of the sensitivity of τ_I to small changes in aspect ratio was made with the intention of determining whether this shift could be explained by uncertainties in aspect ratio measurements. In Figure 5, τ_I vs b^2/a^2 curves are shown for c/a greater and less than the experimental aspect ratio by 1/2 percent. For the less viscous fluid, the curves bracket the data; the apparent discrepancy between the experimental and theoretical peaks is not significant.

For liquid #2, the conclusion is not as definite. A positive correction of 1/2 percent to the aspect ratio brings the theoretical and experimental values of τ_I into closer agreement, including the positions of the peaks; however, the theoretical curve exhibits considerably more asymmetry about the peak than do the data.

C. Results of D'Amico, Kitchens, and Frasier

The quantities τ_n and L were not recorded for these experiments. Fortunately, the ring combinations used were recorded, and all of the rings, rotor, and cylinder are extant, so that measurements could be made of L. However, T (or equivalently, $\tau_n = L/T$) corresponding to the experimental conditions could not be determined because the location of the counterweight used to adjust the position of the center of gravity of the gyroscope was not recorded.

In a particular set of experiments, L and τ_n were varied for each case, so that $\tau_n = \tau_n(L)$. Since the τ_n's in these experiments were not recorded, τ_R and τ_I could not be evaluated by Eqs. (13) and (14) explicitly in terms of measured τ_n. The relationship $\tau_n(L)$ was produced indirectly by solving Eq. (13) numerically for τ_n for all pairs of measured L and τ_R, and fairing curves through the plotted τ_n vs L points. In most cases, one straight line fitted the points quite well, the r.m.s. error of L about the line being about 1/2% of the mean. These points correspond to changes in the increment rings only (see Appendix B). In two experiments, however, the main ring was changed to extend the range of L, producing a discontinuity in the τ_n vs L curve; in these cases the points were fitted with two straight lines, one for each main ring. This fit led to discontinuities in the curves of τ_I vs τ_R (Figs. 6 and 7).

Values of τ_R and τ_I were then evaluated by Eqs. (13) and (14) for each series of L's employed in the experiments, and plots of τ_I vs τ_R were drawn, which could be compared directly with experiment. These plots do not provide a total check of the theory, since part of the input (τ_n) was based on the prior assumption of the theory's validity.

It was stated in Section I that Frasier's comparison of his data[8] to the theory was flawed; the nature of the flaw is now clear. Since neither τ_n nor L was measured during his experiments (except that a single "nominal" L was noted), he could not have correctly evaluated Eq. (14) to find τ_I. It seems likely that he did what later experimenters did; namely, use τ_R in place of τ_n in Eq. (14).

Figs. 6 to 10 present plots of $-\tau_I$ vs τ_R for all of the experiments, including four different liquids at 79% fill, two liquids at 100% fill, and three liquids in a rodded cylinder. The error bars indicate ± 2% error in τ_R and ± 3% error in τ_I. General comments about the agreement between theory and experiment are that: (1) the amplitude at the peak value of τ_I agrees to within 10% when Re $\geqslant 4 \times 10^4$; (2) the amplitude at the peak agrees within 25% at lower Reynolds numbers; (3) in general, the theory predicts a more rapid decay away from the peak than was observed, particularly to the right of the peak. In most of the figures, there is a suggestion of a shifting of the predicted peak response to the left or to the right of the observed peak. However, Fig. 11, showing the effect of a ± 1/2% change in aspect ratio on two of the curves, demonstrates that the apparent shifts are not significant.

IV. CONCLUDING REMARKS

Renewed emphasis is currently being placed on research into the dynamics of liquid-filled shell, in particular by means of gyroscope experiments. In the planning of future work, it is necessary to have a clear picture of what has been accomplished in the past. Examination of available records and reports has revealed inadequacies in the results of previous investigators, such as incomplete recording of data (e.g., moments of inertia) and misleading comparisons of theoretical and experimental results. This report was written in an effort to provide a correct and unified picture of past work.

Comparisons show that predicted and measured frequencies of greatest instability of motion agree to within the experimental error; the growth rates at those frequencies agree to within 10% for Re $> 10^4$, and to within 25% for lower Reynolds number. All work discussed here was performed with the liquid completely spun-up; i.e., in rigid body rotation. The conclusions in Ref. 9 based on this work are valid; namely, that free-oscillation frequencies of the liquid are well-predicted by the Stewartson-Wedemeyer theory, and that coning frequencies and yaw growth rates near resonance agree qualitatively with theoretical predictions. However, the experiments on which these conclusions are based cover only a small range of coning frequencies, ratios of liquid mass to solid mass, and aspect ratios, and, additionally, only a single rotation speed. Also, no direct measurement has been made of the motion of the liquid. Therefore, further work is required in this area to obtain a more distinct quantitative picture of the effect of the liquid on the stability of the shell.

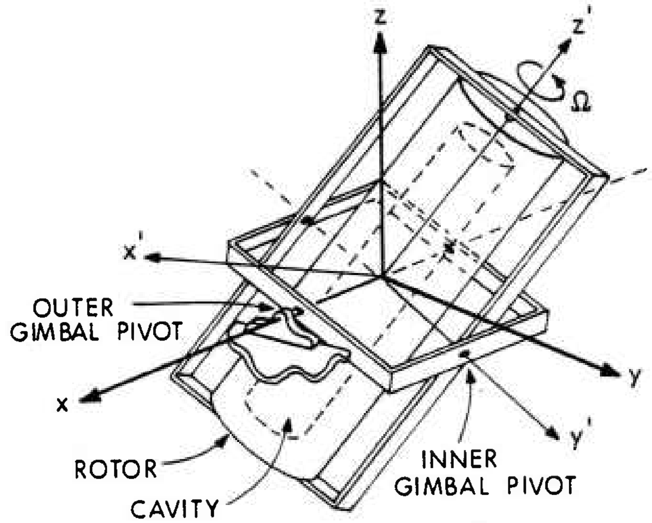

Figure 1. Schematic Diagram of Gyroscope

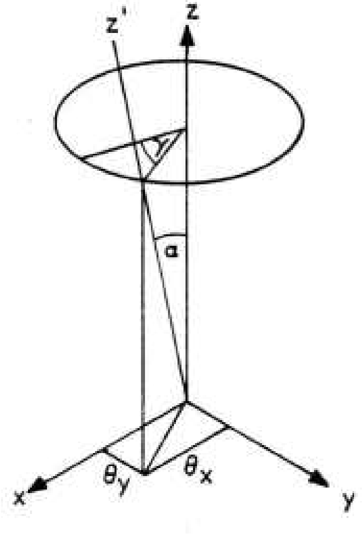

Figure 2. Schematic Diagram of Coordinates

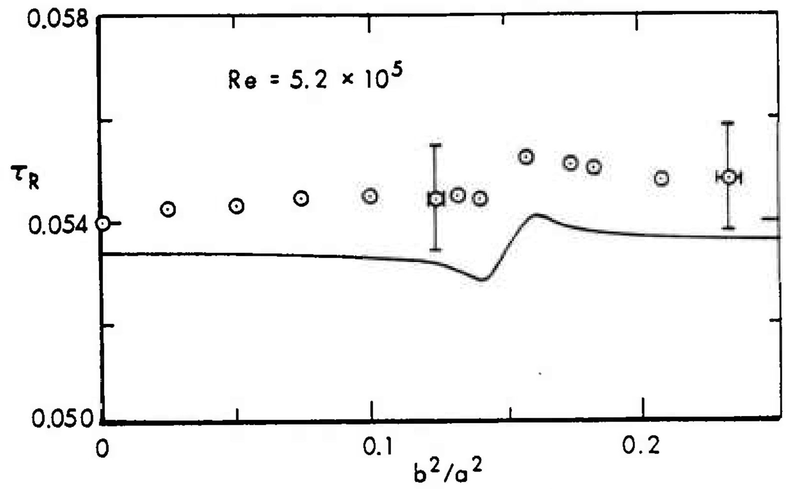

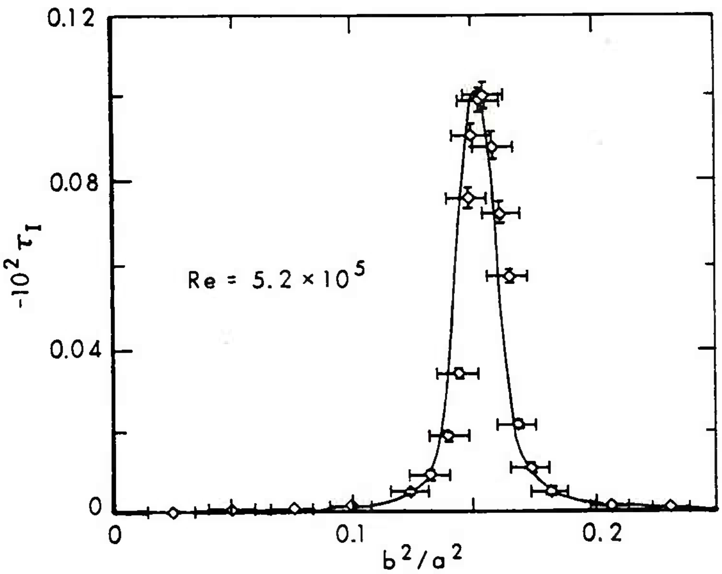

Figure 3. Coning Frequencies and Yaw Growth Rates for Karpov Liquid #1 Experiments ($a = 3.150$ cm, $c = 9.691$ cm, $\rho = 0.818$ g/cm^3, $L = 1.968 \times 10^5$ g cm^2, $\nu = 0.01$ cm^2/s, $\tau_n = 0.0534$; $n = 1$, $j = 1$)

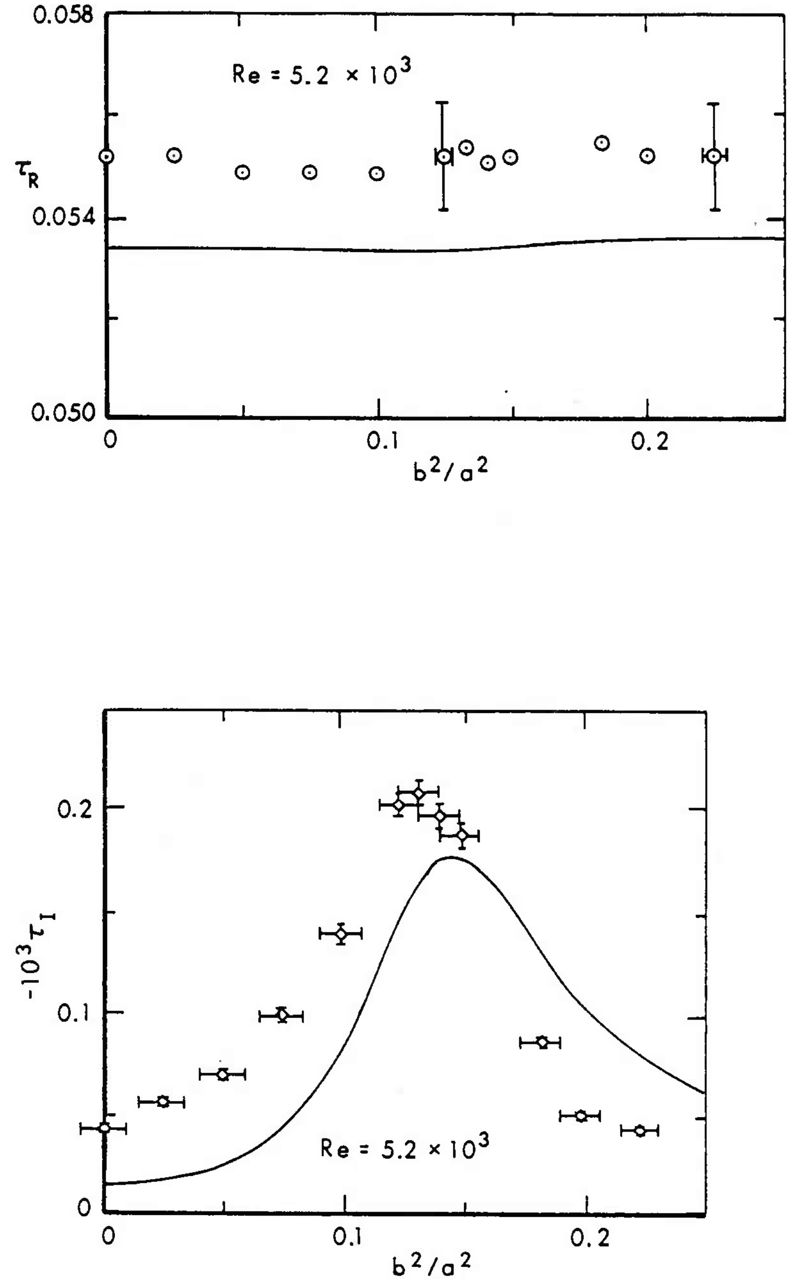

Figure 4. Coning Frequencies and Yaw Growth Rates for Karpov Liquid #2 Experiments ($a = 3.150$ cm, $c = 9.691$ cm, $\rho = 0.818$ g/cm^3, $L = 1.968 \times 10^5$ g cm^2, $\nu = 1.00$ cm^2/s, $\tau_n = 0.0534$; $n = 1$, $j = 1$)

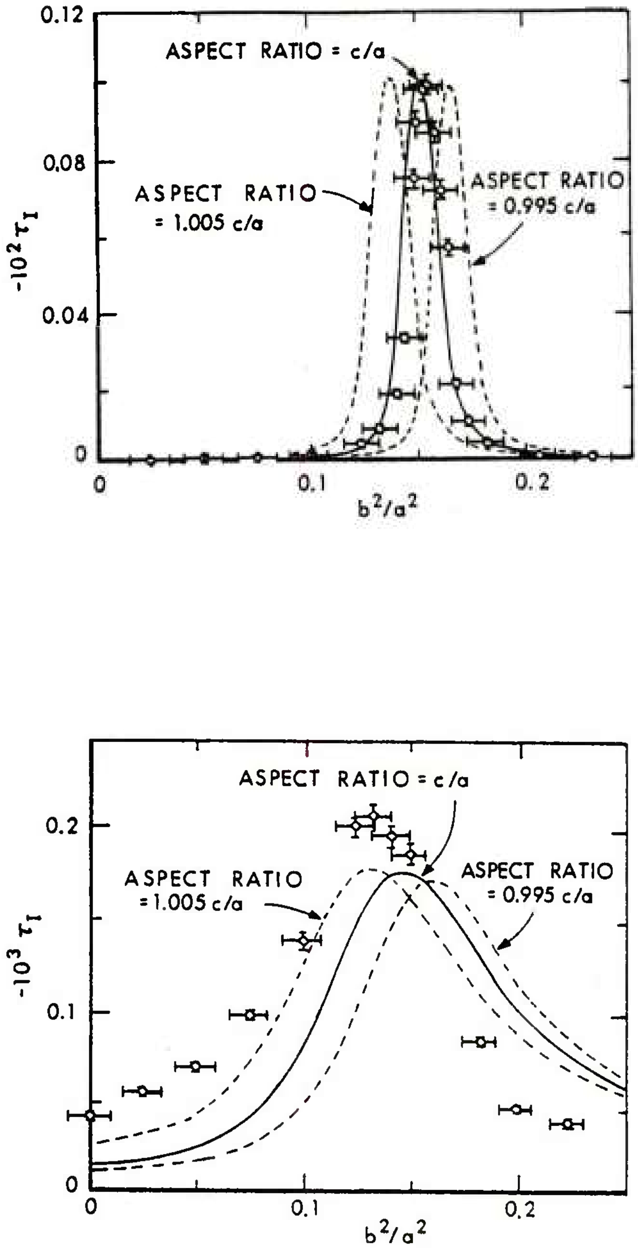

Figure 5. Sensitivity of Yaw Growth Rate to Change in Cylinder Aspect Ratio in Karpov's Experiments (a = 3.150 cm, c = 9.691 cm, $L = 1.968 \times 10^5$ g cm^2, τ_n = 0.0534; n = 1, j = 1)

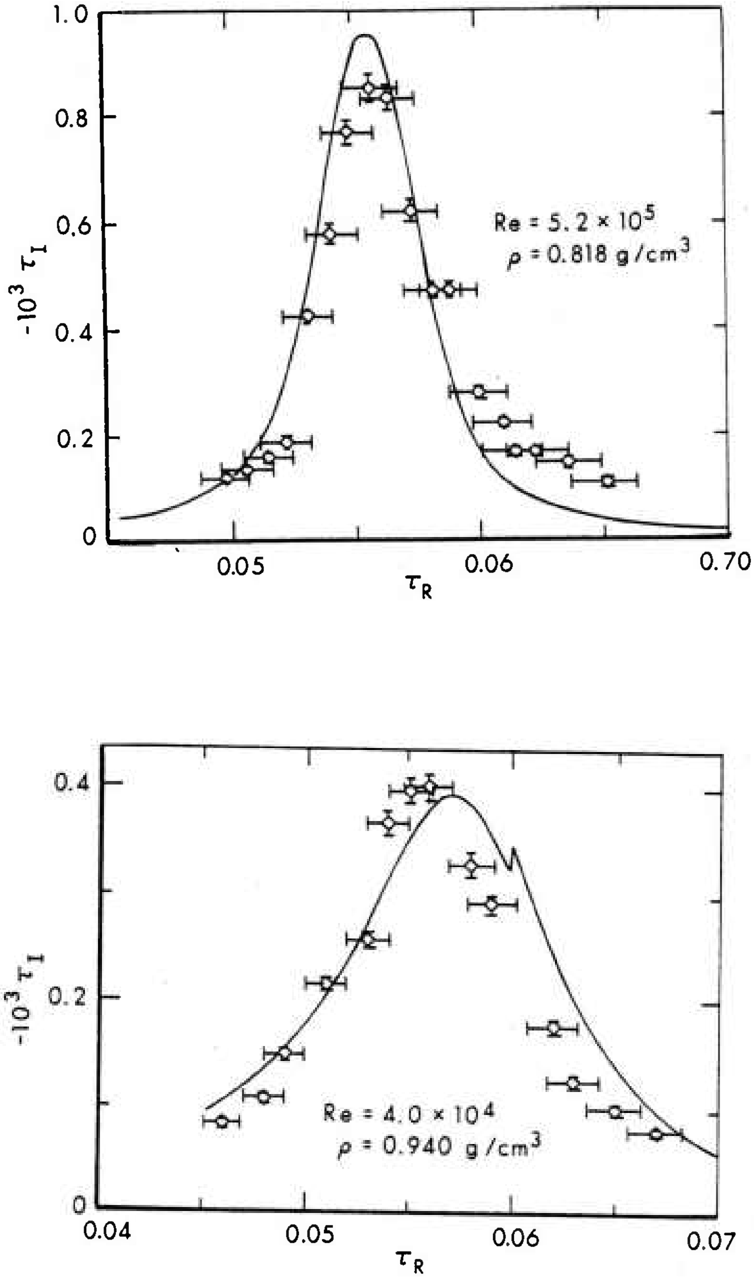

Figure 6. $-\tau_I$ vs τ_R for D'Amico's 79% Filled Cylinder Experiments, Re = 5.2×10^5 and Re = 4.0×10^4 (a = 3.153 cm, c = 9.500 cm, $(b/a)^2 = 0.210$; n = 1, j = 1)

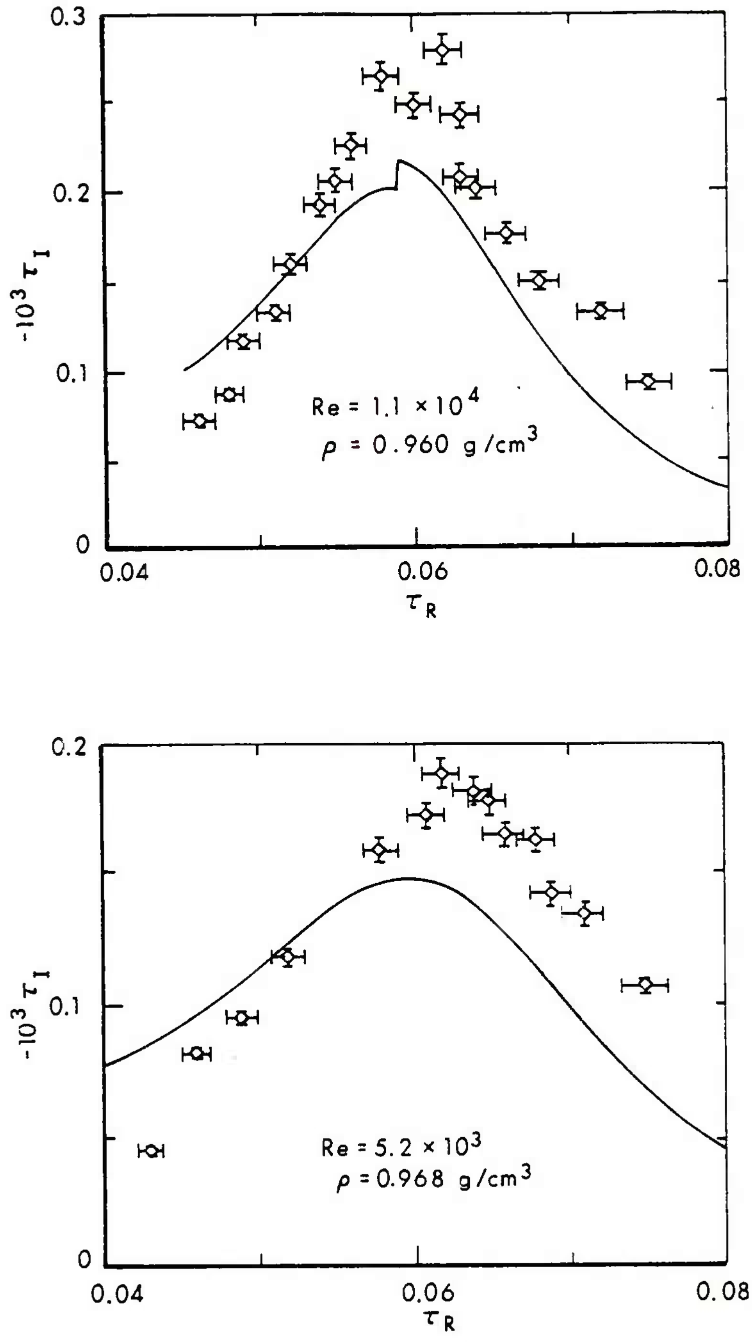

Figure 7. - τ_I vs τ_R for D'Amico's 79% Filled Cylinder Experiments, Re = 1.1 × 10^4 and Re = 5.2 × 10^3 (a = 3.153 cm, c = 9.500 cm, $(b/a)^2$ = 0.210; n = 1, j = 1)

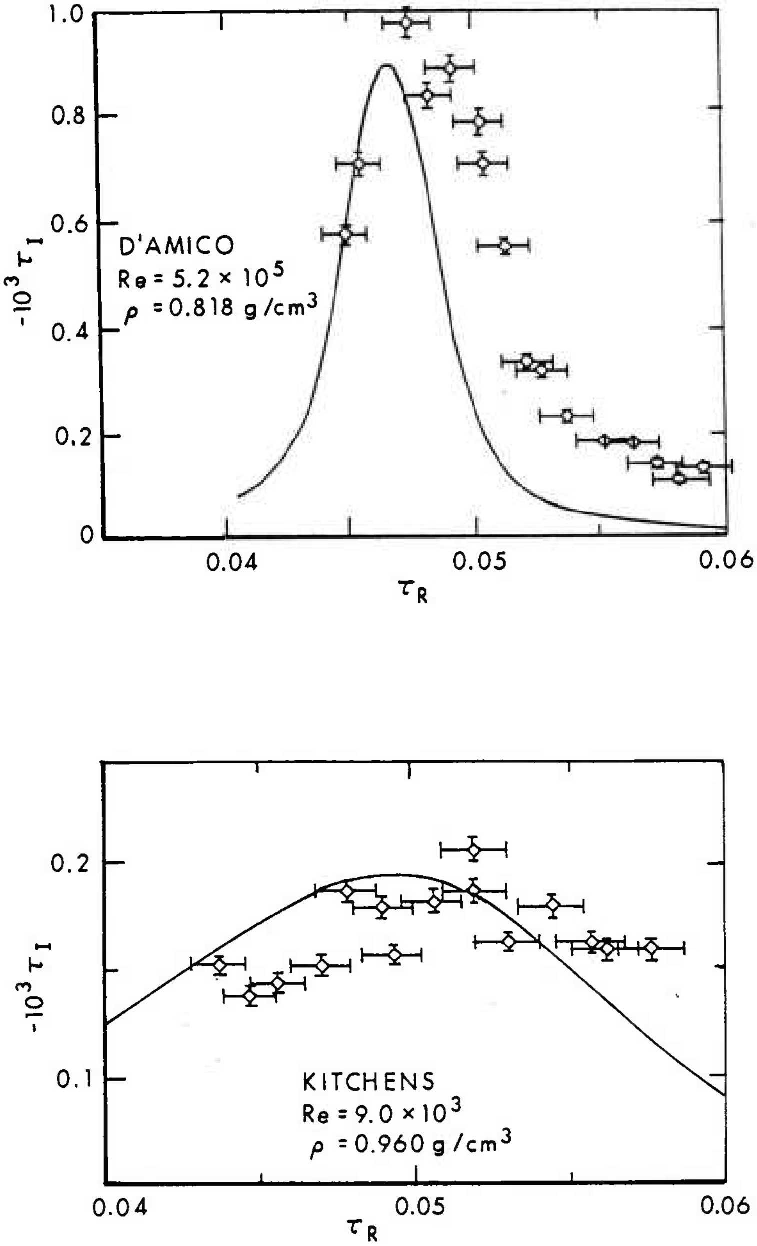

Figure 8. $-\tau_I$ vs τ_R for 100% Filled Cylinders, Experiments of D'Amico and Kitchens (a = 3.153 cm, c = 9.928 cm; n = 1, j = 1)

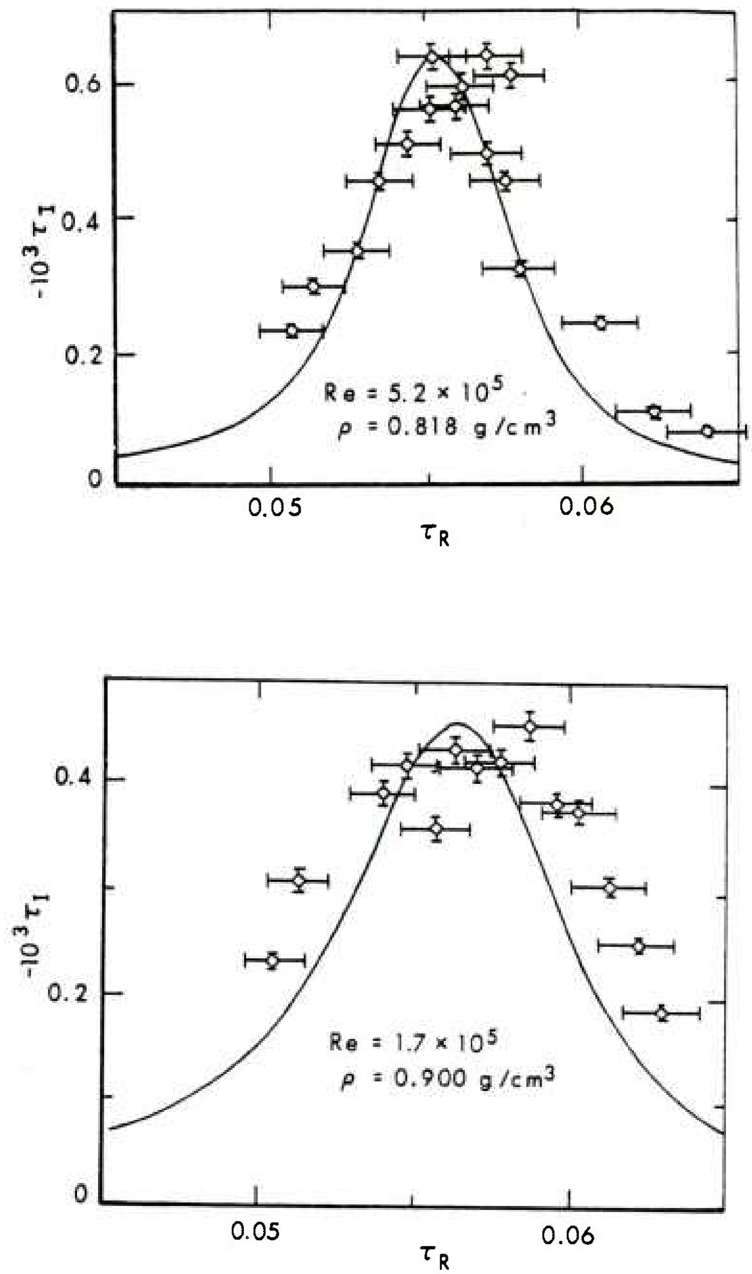

Figure 9. - τ_I vs τ_R for Frasier (Rod) Experiments, Re = 5.2×10^5 and Re = 1.70×10^5 (a = 3.153 cm, c = 9.030 cm, $(d/a)^2$ = 0.023; n = 1, j = 1)

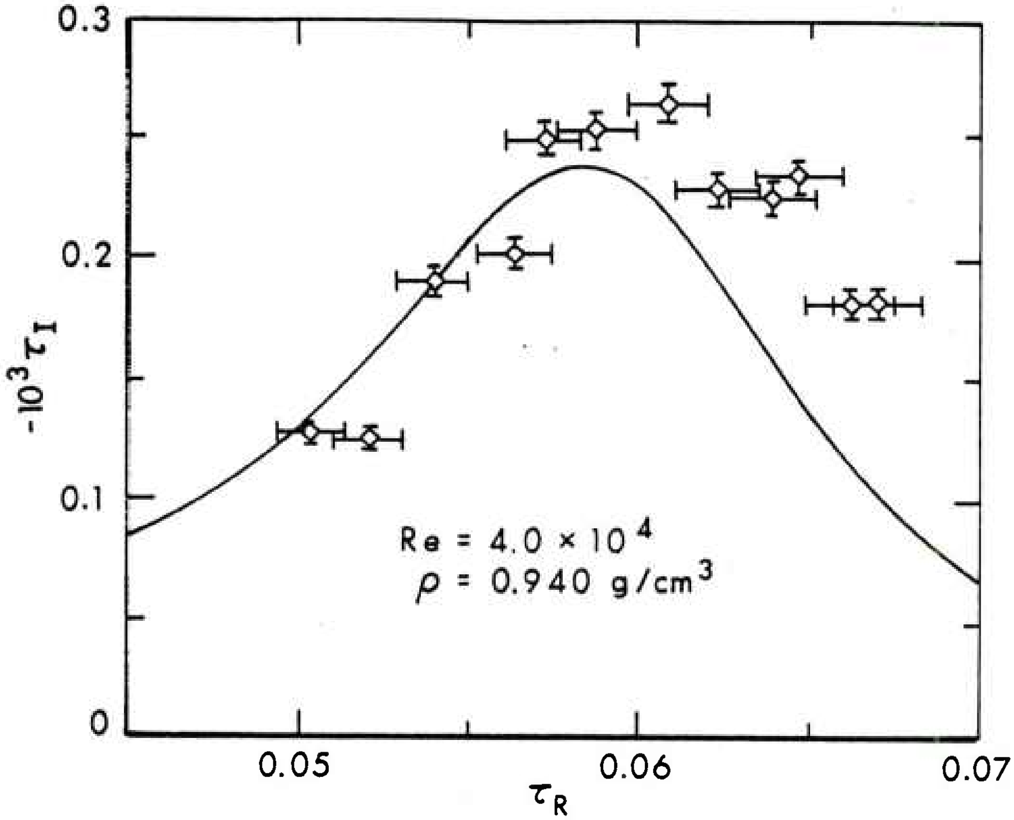

Figure 10. - τ_I vs τ_R for Frasier (Rod) Experiments, Re = 4.0×10^4 (a = 3.153 cm, c = 9.030 cm, $(d/a)^2$ = 0.023; n = 1, j = 1)

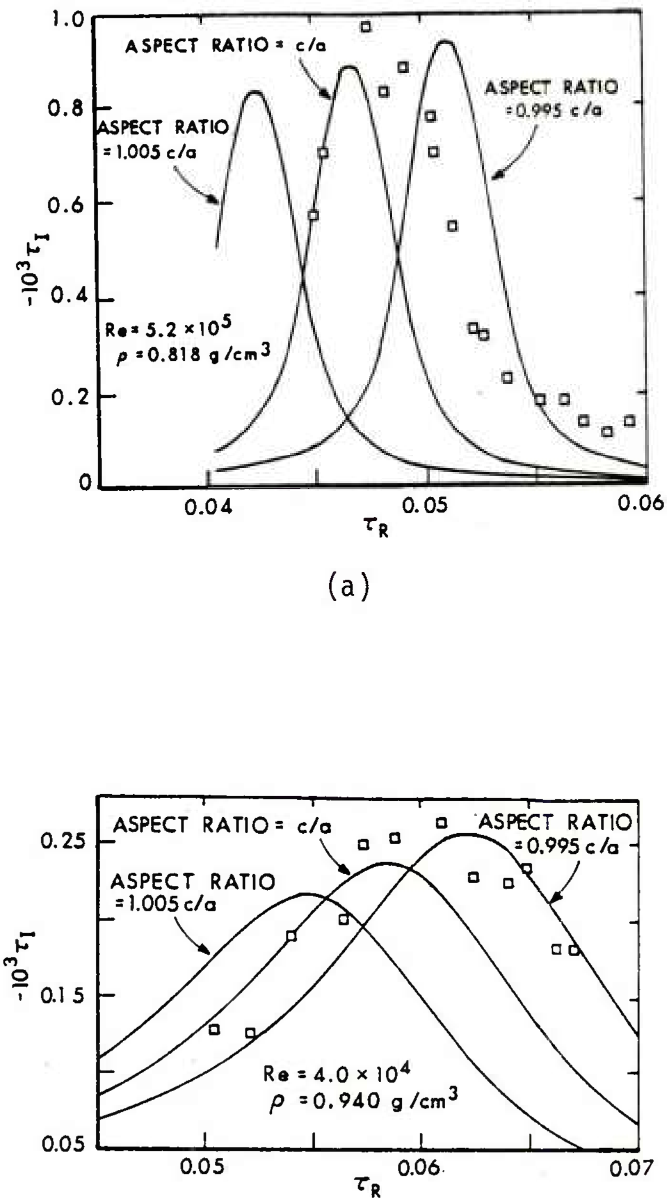

Figure 11. Sensitivity of $-\tau_I$ vs τ_R Curves to Change in Cylinder Aspect Ratio: (a) D'Amico 100% Filled Cylinder, a = 3.153 cm, c = 9.928 cm, j = 1, n = 1; (b) Frasier Cylinder With Inner Burster, a = 3.153 cm, c = 9.030 cm, $(d/a)^2$ = 0.02, n = 1, j = 1

REFERENCES

1. K. Stewartson, "On the Stability of a Spinning Top Containing Liquid," *J. Fluid Mech.*, Vol. 5, Part 4, September 1959, pp. 577-592.

2. G. N. Ward, Appendix to Reference 1.

3. B. G. Karpov, "Dynamics of a Liquid-Filled Shell: Resonance and the Effects of Viscosity," BRL Report No. 1279, U.S. Army Ballistic Research Laboratory, Aberdeen Proving Ground, Maryland, May 1965. AD 468654.

4. B. G. Karpov, "Liquid Filled Gyroscope: The Effect of Reynolds Number on Resonance," BRL Report No. 1302, U.S. Army Ballistic Research Laboratory, Aberdeen Proving Ground, Maryland, October 1965. AD 479430.

5. E. H. Wedemeyer, "Dynamics of Liquid-Filled Shell: Theory of Viscous Corrections to Stewartson's Stability Problem," BRL Report No. 1287, U.S. Army Ballistic Research Laboratory, Aberdeen Proving Ground, Maryland, June 1965. AD 472474.

6. E. H. Wedemeyer, "Viscous Corrections to Stewartson's Stability Criterion," BRL Report No. 1325, U.S. Army Ballistic Research Laboratory, Aberdeen Proving Ground, Maryland, June 1966. AD 489687.

7. J. T. Frasier and W. E. Scott, "Dynamics of a Liquid-Filled Shell: Cylindrical Cavity With a Central Rod," BRL Report No. 1391, U.S. Army Ballistic Research Laboratory, Aberdeen Proving Ground, Maryland, October 1968. AD 667365.

8. J. T. Frasier, "Dynamics of a Liquid-Filled Shell: Viscous Effects in a Cylindrical Cavity With a Central Rod," BRL Memorandum Report No. 1959, U.S. Army Ballistic Research Laboratory, Aberdeen Proving Ground, Maryland, January 1969. AD 684344.

9. <u>Engineering-Design Handbook, Liquid-Filled Projectile Design</u>, AMC Pamphlet No. 706-165, U.S. Army Materiel Development and Readiness Command, Washington, D. C., April 1969. AD 853719.

10. W. P. D'Amico, "Inertial Mode Corrections for the Large Amplitude Motion of a Liquid-Filled Gyroscope," PhD Thesis, University of Delaware, Newark, Delaware, June 1977.

11. W. E. Scott and W. P. D'Amico, "Amplitude-Dependent Behavior of a Liquid Filled Gyroscope," *J. Fluid Mech.*, Vol. 60, Part 4, October 1973, pp. 751-758.

LIST OF SYMBOLS

a	cross-sectional radius of cylindrical cavity (cm)
b	radial coordinate of free surface in partially-filled cylinder (cm)
c	half-height of cylindrical cavity (cm)
d	cross-sectional radius of inner burster (cm)
D	liquid moment residue function, Eq. (7) (g cm^2)
j	index of axial perturbation mode
L	axial moment of inertia of empty gyroscope (g cm^2)
M_o	moment function due to displacement of center of mass from pivot point, Eq. (1) (g cm^2/s^2)
n	index of radial perturbation mode
R	liquid moment residue function, Eq. (8) (non-dimensional)
Re	($\equiv a\Omega^2/\nu$) Reynolds number (non-dimensional)
t	time (s)
T	transverse moment of inertia of empty gyroscope about axis through pivot point (g cm^2)
x, y, z	laboratory fixed rectangular coordinates, z-axis coinciding with unyawed cylinder axis, Figs. 1 and 2 (cm)
x', y', z'	non-rotating rectangular coordinates, z'-axis coinciding with yawing cylinder axis, Figs. 1 and 2 (cm)
α	coning angle, Fig. 2 (radians)
β	$\equiv 4\ M_o T/(L\Omega)^2$ (non-dimensional)
δ	viscous perturbation decay rate/Ω (non-dimensional)
$\delta a, \delta c, \delta d$	effective changes to a, c, and d due to boundary layers, Eq. (9) (cm)
Γ	liquid moment function of τ in Eq. (3) (g cm^2/s^2)
$\overset{*}{\Gamma}$	liquid moment function in Eq. (1) (g cm^2/s^2)

LIST OF SYMBOLS (continued)

$\theta (\equiv \theta_x + i\theta_y)$	complex yaw (θ_x and θ_y being x and y components, respectively) (non-dimensional)
ν	kinematic viscosity of liquid (cm^2/s)
ρ	density of liquid (g/cm^3)
σ	$\equiv (1 - \beta)^{\frac{1}{2}}$
$\tau (\equiv \tau_R + i\tau_I)$	exponent term in exponential solution, Eq. (2)
τ_o	inviscid perturbation eigenfrequency/Ω (non-dimensional)
τ_{oo}	viscous perturbation eigenfrequency/Ω (non-dimensional)
τ_{ov}	$\equiv \tau_{oo} + i\ \delta$, Eq. (10)
τ_I	- (yaw growth rate)/Ω (non-dimensional)
τ_n	nutational frequency of empty gyroscope/Ω, Eq. (4) (non-dimensional)
τ_p	precessional frequency of empty gyroscope/Ω, Eq. (4) (non-dimensional)
τ_R	coning frequency of liquid-filled gyroscope (non-dimensional)
Ω	spin rate of cylinder (radians/s)

APPENDIX A: DERIVATION OF EQUATIONS (13) AND (14)

We start with Eq. (6-2) of Ref. 9:

$$\tau = (1/2)(\tau_n + \tau_{ov}) \pm \{[(1/2)(\tau_n - \tau_{ov})]^2 - |D|/(\sigma L)\}^{1/2} \qquad (A.1)$$

Recalling that $\tau_{ov} = \tau_{oo} + i\delta$, Eq. (A.1) can be written

$$\tau = (1/2)(\tau_n + \tau_{oo}) + (1/2)i\delta \pm (1/2)i \;\{(4|D|)/(\sigma L) + \delta^2 - (\tau_n - \tau_{oo})^2 + 2i\delta\,(\tau_n - \tau_{oo})\}^{1/2} \qquad (A.2)$$

If we now define

$$m = (4|D|)/(\sigma L) + \delta^2 - (\tau_n - \tau_{oo})^2$$

and $$\tilde{n} = 2\,\delta\,(\tau_n - \tau_{oo}),$$

where $m>0$ for the ranges of parameters considered. Eq. (A.2) can be written

$$\tau = (1/2)(\tau_n + \tau_{oo}) + (1/2)i\delta \pm (1/2)i\,(m + i\tilde{n})^{1/2} \qquad (A.3)$$

This corresponds to Eq. (6-6) in Ref. 9, with $\tilde{n}$ replacing n. Note that Eq. (6-6) of the reference is in error, given the definition of n there.

Let $$m + i\,\tilde{n} \equiv \lambda\, e^{i\theta} \quad , \qquad (A.4)$$

where

$$\lambda^2 = m^2 + n^2 \;, \quad \theta = \tan^{-1}(\tilde{n}/m) \;, \quad \operatorname{sgn}(\theta) = \operatorname{sgn}(\tilde{n}) \;, \quad -\pi < \theta < \pi \;. \qquad (A.5)$$

Then

$$\pm\, i\,(m + i\,\tilde{n})^{1/2} = \pm\,\lambda^{1/2}\,[-\sin(\theta/2) + i\cos(\theta/2)] \quad .$$

For $$-\pi/2 < \theta/2 < \pi/2 \quad ,$$

$$\sin(\theta/2) = \operatorname{sgn}(\theta)\;[(1 - \cos\theta)/2]^{1/2} \quad ,$$

and $$\cos(\theta/2) = [(1 + \cos\theta)/2]^{1/2} \quad .$$

Thus

$$\pm\, i\,(m + i\,\tilde{n})^{1/2} = \pm\,\lambda^{1/2}\,[-\mathrm{sgn}(\theta)\,\{(1 - \cos\theta)/2\}^{1/2}$$

$$+\, i\,\{(1 + \cos\theta)/2\}^{1/2}] \quad . \qquad (A.6)$$

Using the following trigometric identity:

$$\cos(\tan^{-1} x) = (1 + x^2)^{-1/2} \quad \text{for} \quad -\pi/2 < \tan^{-1} x < \pi/2 \ ,$$

and Eq. (A.5), we get

$$\pm\, i\,(m + i\,\tilde{n})^{1/2} = \pm\, 2^{-1/2}\,[-\mathrm{sgn}(\tilde{n})\,\{(m^2 + \tilde{n}^2)^{1/2} - m\}^{1/2}$$

$$+\, i\,\{(m^2 + \tilde{n}^2)^{1/2} + m\}^{1/2}] \quad . \qquad (A.7)$$

Inserting Eq. (A.7) into Eq. (A.3) and separating real and imaginary parts, we get

$$\tau_R = (1/2)(\tau_n + \tau_{oo}) \mp (1/2)\,\mathrm{sgn}(\tilde{n})\,[\{(m^2 + \tilde{n}^2)^{1/2} - m\}/2]^{1/2}$$

$$\tau_I = (1/2)\delta \pm (1/2)[\{(m^2 + \tilde{n}^2)^{1/2} + m\}/2]^{1/2} \quad , \qquad (A.8)$$

which are Eqs. (13) and (14) in this report.

APPENDIX B. DATA FROM EXPERIMENTS

For the convenience of future investigators, relevant data from the experiments described in this report are tabulated here. All frequencies and growth rates listed here were obtained by the original researchers from the raw data; no re-reduction of raw data was performed by the present authors, except to verify the reduction methods.

In all experiments except those of Karpov, the axial moment of inertia of the gyroscope was varied by changing rings mounted on the rotor. These rings were of two types: main rings, in five sizes; and increment rings, in four sizes. At any one time, only one main ring was used, but any or all increment rings could be used. The increment rings were mounted above or below the main rings, the two positions being distinguished as "top" and "bottom" in the experimental records. The axial moments of inertia of the components of the gyroscope were measured by the present authors and are shown in Table B-1, together with the corresponding masses. There were three increment rings of size .001 and two of each of the other sizes. The values shown in Table B-1 represent mean values of the rings of each size.

TABLE B-1. AXIAL MOMENT OF INERTIA OF GYROSCOPE COMPONENTS

Component	Mass (g)	Axial Moment of Inertia (g cm^2)
Steel Rotor	2554	3.221×10^4
Plastic Cylinder	933	0.841
Main Ring 1	1650	6.238
Main Ring 2	3160	13.87
Main Ring 3	4455	21.74
Main Ring 4	6510	31.03
Main Ring 5	7725	39.22
Increment Ring .001	180	0.48
Increment Ring .002	309	0.93
Increment Ring .0025	367	1.10
Increment Ring .005	615	2.12

In the experimental records, numbers are given which indicate the total "value" of the increment rings used. For example, in one case the increments might be recorded as "top-.003, bottom-.005". This could represent any of the combinations shown in Table B-2. Unfortunately, not all of the combinations have the same axial moment of inertia. In this work, wherever there were several possible increment combinations, the mean moment of inertia of the combinations was used. In the worst case, this led to an inaccuracy of less than one percent of the total axial moment of inertia of the gyroscope.

TABLE B-2. INCREMENT RING COMBINATIONS WHICH COULD BE LISTED AS "TOP-.003, BOTTOM-.005"

Top Increments	Bottom Increments	Total Axial M.O.I. of Increments (g cm^2)
.001 , .002	.005	3.53×10^4
.001 , .002	2 × .0025	3.62×10^4
3 × .001	.005	3.56×10^4
3 × .001	2 × .0025	3.65×10^4
	Mean	3.59×10^4

In the following tables, the data describing each experiment are presented. The date indicated for each experiment is approximate.

TABLE B-3. THE EXPERIMENT OF KARPOV (1965)

	$a = 3.150$ cm	$c = 9.691$ m
	$\tau_n = 0.0534$	$L = 1.968 \times 10^5$ g cm^2
	$\nu = 0.01$ cm^2/s	$\nu = 1.0$ cm^2/s
	$\rho = 0.818$ g/cm^3	$\rho = 0.968$ g/cm^3

b^2/a^2	τ_R	$-\tau_I$	τ_R	$-\tau_I$
0	.0540		.0552	$.439 \times 10^{-4}$
.0248	.0542	$.038 \times 10^{-4}$	.0552	.573
.0496	.0543	.076	.0548	.707
.0744	.0545	.115	.0549	.993
.0992	.0545	.153	.0549	1.394
.1240	.0544	.458	.0552	2.024
.1322	.0545	.917	.0554	2.082
.1405	.0544	1.872	.0551	1.967
.1446		3.400		
.1488		7.563	.0552	1.872
.1504		9.015		
.1537		9.855		
.1554		9.969		
.1570	.0552			
.1587		8.747		

TABLE B-3. THE EXPERIMENT OF KARPOV (1965) (continued)

b^2/a^2	τ_R	$-\tau_I$	τ_R	$-\tau_I$
.1620		7.219×10^{-4}		
.1653		5.691		
.1686		2.139		
.1736	.0551	1.070		
.1818	.0550	.477	.0555	$.859 \times 10^{-4}$
.1983			.0552	.497
.2066	.0548	.095		
.2231			.0552	.420
.2314	.0548	.038		

TABLE B-4. THE EXPERIMENT OF D'AMICO (1969)

a = 3.153 cm c = 9.500 cm $b^2/a^2 = 0.21$

$\nu = 0.01$ cm^2/s , $\rho = 0.818$ g/cm^3

Main Ring	Increment Rings Top	Increment Rings Bottom	L(g cm^2)	τ_R	$-\tau_I$
2	0.0000	0.0010	1.878E+05	0.0498	1.222E-04
2	0.0010	0.0010	1.926E+05	0.0507	1.375E-04
2	0.0020	0.0010	1.973E+05	0.0515	1.623E-04
2	0.0020	0.0020	2.018E+05	0.0522	1.891E-04
2	0.0025	0.0025	2.051E+05	0.0532	4.259E-04
2	0.0025	0.0035	2.099E+05	0.0542	5.806E-04
2	0.0035	0.0035	2.147E+05	0.0549	7.678E-04
2	0.0045	0.0035	2.193E+05	0.0558	8.537E-04
2	0.0040	0.0050	2.234E+05	0.0565	8.346E-04
2	0.0050	0.0050	2.276E+05	0.0574	6.226E-04
2	0.0050	0.0060	2.320E+05	0.0582	4.698E-04
2	0.0060	0.0060	2.368E+05	0.0589	4.736E-04
2	0.0060	0.0070	2.402E+05	0.0600	2.827E-04
2	0.0070	0.0070	2.448E+05	0.0610	2.215E-04
2	0.0075	0.0075	2.494E+05	0.0614	1.719E-04
2	0.0085	0.0075	2.537E+05	0.0623	1.700E-04
2	0.0085	0.0095	2.617E+05	0.0636	1.490E-04
2	0.0105	0.0095	2.711E+05	0.0651	1.089E-04

TABLE B-4. THE EXPERIMENT OF D'AMICO (1969) (continued)

$\nu = 0.13\ cm^2/s$ $\rho = 0.940\ g/cm^3$

Main Ring	Increment Rings Top	Increment Rings Bottom	$L(g\ cm^2)$	τ_R	$-\tau_I$
2	0.0000	0.0020	1.925E+05	0.0460	8.594E-05
2	0.0020	0.0020	2.018E+05	0.0480	1.089E-04
2	0.0060	0.0000	2.100E+05	0.0490	1.509E-04
2	0.0060	0.0020	2.189E+05	0.0510	2.177E-04
2	0.0050	0.0050	2.276E+05	0.0530	2.597E-04
2	0.0070	0.0050	2.365E+05	0.0540	3.686E-04
2	0.0070	0.0070	2.448E+05	0.0550	3.992E-04
2	0.0075	0.0085	2.537E+05	0.0560	4.030E-04
2	0.0095	0.0085	2.617E+05	0.0580	3.304E-04
2	0.0105	0.0095	2.711E+05	0.0590	2.941E-04
3	0.0000	0.0000	2.620E+05	0.0620	1.776E-04
3	0.0000	0.0020	2.715E+05	0.0630	1.261E-04
3	0.0020	0.0020	2.808E+05	0.0650	9.931E-05
3	0.0000	0.0060	2.890E+05	0.0670	8.021E-05

$\nu = 0.49\ cm^2/s$, $\rho = 0.960\ g/cm^3$

Main Ring	Increment Rings Top	Increment Rings Bottom	$L(g\ cm^2)$	τ_R	$-\tau_I$
2	0.0020	0.0020	2.018E+05	0.0460	7.257E-05
2	0.0010	0.0050	2.100E+05	0.0480	8.785E-05
2	0.0030	0.0050	2.189E+05	0.0490	1.165E-04
2	0.0050	0.0050	2.276E+05	0.0510	1.337E-04
2	0.0070	0.0050	2.365E+05	0.0520	1.604E-04
2	0.0070	0.0070	2.448E+05	0.0540	1.929E-04
2	0.0085	0.0075	2.537E+05	0.0550	2.063E-04
2	0.0085	0.0095	2.617E+05	0.0560	2.254E-04
2	0.0105	0.0095	2.711E+05	0.0580	2.655E-04
3	0.0000	0.0000	2.620E+05	0.0600	2.483E-04
3	0.0000	0.0020	2.715E+05	0.0620	2.807E-04
3	0.0020	0.0020	2.808E+05	0.0630	2.426E-04
3	0.0000	0.0035	2.778E+05	0.0630	2.082E-04
3	0.0020	0.0035	2.873E+05	0.0640	2.024E-04
3	0.0040	0.0035	2.966E+05	0.0660	1.776E-04
3	0.0030	0.0070	3.073E+05	0.0680	1.509E-04
3	0.0070	0.0070	3.238E+05	0.0720	1.337E-04
3	0.0095	0.0105	3.501E+05	0.0750	9.358E-05

TABLE B-4. THE EXPERIMENT OF D'AMICO (1969) (continued)

$\nu = 1.0\ cm^2/s$, $\rho = 0.968\ g/cm^3$

Main Ring	Increment Rings Top	Bottom	L(g cm^2)	τ_R	$-\tau_I$
2	0.0000	0.0000	1.830E+05	0.0430	4.584E-05
2	0.0020	0.0020	2.018E+05	0.0460	8.212E-05
2	0.0045	0.0035	2.193E+05	0.0490	9.549E-05
2	0.0060	0.0060	2.368E+05	0.0520	1.184E-04
2	0.0075	0.0085	2.537E+05	0.0580	1.585E-04
2	0.0095	0.0105	2.711E+05	0.0610	1.719E-04
3	0.0000	0.0020	2.715E+05	0.0620	1.891E-04
3	0.0020	0.0020	2.808E+05	0.0640	1.814E-04
3	0.0025	0.0035	2.889E+05	0.0650	1.776E-04
3	0.0045	0.0035	2.983E+05	0.0660	1.642E-04
3	0.0050	0.0050	3.066E+05	0.0680	1.623E-04
3	0.0050	0.0070	3.155E+05	0.0690	1.413E-04
3	0.0070	0.0070	3.238E+05	0.0710	1.337E-04
3	0.0105	0.0095	3.501E+05	0.0750	1.070E-04

TABLE B-5. THE EXPERIMENT OF D'AMICO (1974)

a = 3.153 cm c = 9.928 cm $b^2/a^2 = 0$

$\nu = 0.01\ cm^2/s$, $\rho = 0.818\ g/cm^3$

Main Ring	Top	Bottom	L(g cm^2)	τ_R	$-\tau_I$
2	0.0000	0.0000	1.830E+05	0.0450	5.730E-04
2	0.0010	0.0000	1.878E+05	0.0456	7.066E-04
2	0.0010	0.0010	1.926E+05	0.0476	9.778E-04
2	0.0020	0.0010	1.973E+05	0.0484	8.346E-04
2	0.0020	0.0020	2.018E+05	0.0493	8.862E-04
2	0.0020	0.0030	2.066E+05	0.0504	7.811E-04
2	0.0020	0.0030	2.066E+05	0.0506	7.028E-04
2	0.0030	0.0030	2.112E+05	0.0514	5.500E-04
2	0.0035	0.0035	2.147E+05	0.0523	3.304E-04
2	0.0035	0.0045	2.193E+05	0.0528	3.151E-04
2	0.0050	0.0050	2.276E+05	0.0538	2.292E-04
2	0.0050	0.0060	2.320E+05	0.0553	1.814E-04
2	0.0060	0.0060	2.368E+05	0.0564	1.757E-04
2	0.0060	0.0070	2.402E+05	0.0573	1.375E-04
2	0.0070	0.0070	2.448E+05	0.0583	1.089E-04
2	0.0070	0.0080	2.496E+05	0.0593	1.318E-04

TABLE B-6. THE EXPERIMENT OF KITCHENS (1976)

$a = 3.153$ cm $\qquad$ $c = 9.928$ cm $\qquad$ $b^2/a^2 = 0$

$\nu = 0.58\ cm^2/s$, $\qquad$ $\rho = 0.960\ g/cm^3$

Main Ring	Increment Rings Top	Bottom	$L(g\ cm^2)$	τ_R	$-\tau_I$
2	0.0000	0.0010	1.878E+05	0.0437	1.53E-04
2	0.0000	0.0020	1.925E+05	0.0447	1.39E-04
2	0.0010	0.0020	1.973E+05	0.0456	1.45E-04
2	0.0020	0.0020	2.018E+05	0.0470	1.53E-04
2	0.0030	0.0020	2.066E+05	0.0478	1.88E-04
2	0.0030	0.0030	2.112E+05	0.0490	1.80E-04
2	0.0020	0.0050	2.147E+05	0.0493	1.58E-04
2	0.0030	0.0050	2.189E+05	0.0506	1.83E-04
2	0.0040	0.0050	2.234E+05	0.0519	2.08E-04
2	0.0050	0.0050	2.276E+05	0.0519	1.88E-04
2	0.0050	0.0060	2.320E+05	0.0530	1.64E-04
2	0.0060	0.0060	2.368E+05	0.0544	1.81E-04
2	0.0070	0.0060	2.402E+05	0.0557	1.64E-04
2	0.0070	0.0070	2.448E+05	0.0562	1.61E-04
2	0.0080	0.0070	2.496E+05	0.0576	1.61E-04

TABLE B-7. THE EXPERIMENT OF FRASIER (1968)

a = 3.153 cm c = 9.030 cm

Central Rod: $d^2/a^2 = .023$

$\nu = 0.01\ cm^2/s$, $\rho = 0.818\ g/cm^3$

Main Ring	Increment Rings Top	Increment Rings Bottom	L(g cm^2)	τ_R	$-\tau_I$
2	0.0000	0.0000	1.830E+05	0.0507	2.349E-04
2	0.0010	0.0000	1.878E+05	0.0514	2.998E-04
2	0.0010	0.0020	1.973E+05	0.0528	3.533E-04
2	0.0020	0.0020	2.018E+05	0.0536	4.603E-04
2	0.0030	0.0020	2.066E+05	0.0545	5.138E-04
2	0.0025	0.0035	2.099E+05	0.0552	5.615E-04
2	0.0035	0.0025	2.099E+05	0.0553	6.398E-04
2	0.0035	0.0035	2.147E+05	0.0560	5.672E-04
2	0.0035	0.0035	2.147E+05	0.0562	5.940E-04
2	0.0035	0.0045	2.193E+05	0.0570	4.966E-04
2	0.0035	0.0045	2.193E+05	0.0570	6.398E-04
2	0.0045	0.0045	2.239E+05	0.0576	4.584E-04
2	0.0045	0.0045	2.239E+05	0.0578	6.092E-04
2	0.0050	0.0050	2.276E+05	0.0580	3.285E-04
2	0.0060	0.0060	2.368E+05	0.0606	2.464E-04
2	0.0070	0.0070	2.448E+05	0.0623	1.146E-04
2	0.0075	0.0085	2.537E+05	0.0640	8.212E-05

$\nu = 0.03\ cm^2/s$, $\rho = 0.900\ g/cm^3$

Main Ring	Increment Rings Top	Increment Rings Bottom	L(g cm^2)	τ_R	$-\tau_I$
2	0.0000	0.0000	1.830E+05	0.0505	2.311E-04
2	0.0000	0.0010	1.878E+05	0.0513	3.075E-04
2	0.0020	0.0020	2.018E+05	0.0540	3.915E-04
2	0.0025	0.0025	2.051E+05	0.0547	4.183E-04
2	0.0035	0.0025	2.099E+05	0.0557	3.591E-04
2	0.0035	0.0035	2.147E+05	0.0563	4.335E-04
2	0.0035	0.0045	2.193E+05	0.0570	4.163E-04
2	0.0045	0.0045	2.239E+05	0.0578	4.221E-04
2	0.0045	0.0055	2.287E+05	0.0587	4.584E-04
2	0.0050	0.0060	2.320E+05	0.0596	3.820E-04
2	0.0060	0.0060	2.368E+05	0.0603	3.762E-04
2	0.0060	0.0070	2.402E+05	0.0613	3.056E-04
2	0.0070	0.0070	2.448E+05	0.0622	2.502E-04
2	0.0070	0.0075	2.473E+05	0.0630	1.872E-04

TABLE B-7. THE EXPERIMENT OF FRASIER (1963) (continued)

$\nu = 0.13\ cm^2/s$, $\rho = 0.940\ g/cm^3$

Main Ring	Increment Rings Top	Increment Rings Bottom	$L(g\ cm^2)$	τ_R	$-\tau_I$
2	0.0000	0.0000	1.830E+05	0.0504	1.280E-04
2	0.0000	0.0020	1.925E+05	0.0521	1.261E-04
2	0.0020	0.0020	2.018E+05	0.0540	1.910E-04
2	0.0035	0.0025	2.099E+05	0.0564	2.024E-04
2	0.0035	0.0045	2.193E+05	0.0573	2.502E-04
2	0.0050	0.0050	2.276E+05	0.0588	2.540E-04
2	0.0050	0.0070	2.365E+05	0.0609	2.655E-04
2	0.0070	0.0070	2.448E+05	0.0624	2.292E-04
2	0.0075	0.0085	2.537E+05	0.0640	2.254E-04
2	0.0085	0.0085	2.585E+05	0.0648	2.349E-04
2	0.0095	0.0095	2.663E+05	0.0663	1.833E-04
2	0.0105	0.0095	2.711E+05	0.0671	1.833E-04

DISTRIBUTION LIST

No. of Copies	Organization
12	Commander Defense Technical Info Center ATTN: DDC-DDA Cameron Station Alexandria, VA 22314
1	Commander US Army Engineer Waterways Experiment Station ATTN: R. H. Malter Vicksburg, MS 39180
1	Commander US Army Materiel Development and Readiness Command ATTN: DRCDMD-ST 5001 Eisenhower Avenue Alexandria, VA 22333
3	Commander US Army Armament Research and Development Command ATTN: DRDAR-TSS (2 cys) DRDAR-LC, Dr. J.Frasier Dover, NJ 07801
6	Commander US Army Armament Research and Development Command ATTN: DRDAR-LCA-F Mr. D. Mertz Mr. E. Falkowski Mr. A. Loeb Mr. R. Kline Mr. S. Kahn Mr. S. Wasserman Dover, NJ 07801
1	Commander US Army Armament Materiel Readiness Command ATTN: DRSAR-LEP-L, Tech Lib Rock Island, IL 61299
1	Director US Army ARRADCOM Benet Weapons Laboratory ATTN: DRDAR-LCB-TL Watervliet, NY 12189
1	Commander US Army Aviation Research and Development Command ATTN: DRSAV-E P. O. Box 209 St. Louis, MO 63166
1	Director US Army Air Mobility Research and Development Laboratory ATTN: SAVDL-D, W.J.McCroskey Ames Research Center Moffett Field, CA 94035
1	Commander US Army Communications Rsch and Development Command ATTN: DRDCO-PPA-SA Fort Monmouth, NJ 07703
1	Commander US Army Electronics Research and Development Command Technical Support Activity ATTN: DELSD-L Fort Monmouth, NJ 07703
4	Commander US Army Missile Command ATTN: DRSMI-R DRSMI-YDL DRSMI-RDK Mr. R. Deep Mr. R. Becht Redstone Arsenal, AL 35809

DISTRIBUTION LIST

No. of Copies	Organization
1	Commander US Army Tank Automotive Research & Development Cmd ATTN: DRDTA-UL Warren, MI 48090
1	Commander US Army Jefferson Proving Ground ATTN: STEJP-TD-D Madison, IN 47250
1	Commander US Army Research Office ATTN: Dr. R. E. Singleton P. O. Box 12211 Research Triangle Park NC 27709
1	AGARD-NATO ATTN: R. H. Korkegi APO New York 09777
1	Director US Army TRADOC Systems Analysis Activity ATTN: ATAA-SL, Tech Lib White Sands Missile Range NM 88002
3	Commander Naval Air Systems Command ATTN: AIR-604 Washington, DC 20360
3	Commander Naval Ordnance Systems Command ATTN: ORD-0632 ORD-035 ORD-5524 Washington, DC 20360
2	Commander David W. Taylor Naval Ship Research & Development Cmd ATTN: H. J. Lugt, Code 1802 S. de los Santos Head, High Speed Aero Division Bethesda, MD 20084
1	Commander Naval Surface Weapons Center ATTN: DX-21, Lib Br. Dahlgren, VA 22448
5	Commander Naval Surface Weapons Center Applied Aerodynamics Division ATTN: K. R. Enkenhus M. Ciment S. M. Hastings A. E. Winklemann W. C. Ragsdale Silver Spring, MD 20910
1	AFATL (DLDL, Dr. D.C.Daniel) Eglin AFB, FL 32542
2	AFFDL (W.L. Hankey; J.S.Shang) Wright-Patterson AFB, OH 45433
4	Director National Aeronautics and Space Administration ATTN: D. R. Chapman J. Rakich W. C. Rose B. Wick Ames Research Center Moffett Field, CA 94035

DISTRIBUTION LIST

No. of Copies	Organization
4	Director National Aeronautics and Space Administration ATTN: E. Price J. South J. R. Sterrett Tech Library Langley Research Center Langley Station Hampton, VA 23365
1	Director National Aeronautics and Space Administration Lewis Research Center ATTN: MS 60-3, Tech Lib 21000 Brookpark Road Cleveland, OH 44135
2	Director National Aeronautics and Space Administration Marshall Space Flight Center ATTN: A. R. Felix, Chief S&E-AERO-AE Dr. W. W. Fowlis Huntsville, AL 35812
2	Director Jet Propulsion Laboratory ATTN: L. M. Mack Tech Library 4800 Oak Grove Drive Pasadeno, CA 91103
3	Arnold Research Org., Inc. ATTN: J. D. Whitfield R. K. Matthews J. C. Adams Arnold AFB, TN 37389
3	Aerospace Corporation ATTN: T. D. Taylor H. Mirels R. L. Varwig Aerophysics Lab. P.O. Box 92957 Los Angeles, CA 90009
1	AVCO Systems Division ATTN: B. Reeves 201 Lowell Street Wilmington, MA 01887
3	The Boeing Company Commercial Airplane Group ATTN: W. A. Bissell, Jr. M. S. 1W-82, Org 6-8340 P. E. Rubbert J. D. McLean Seattle, WA 98124
3	Calspan Corporation ATTN: A. Ritter G. Homicz W. Rae P.O. Box 235 Buffalo, NY 14221
1	Center for Interdisciplinary Programs ATTN: Victor Zakkay W. 177th Street & Harlem River Bronx, NY 10453
1	General Dynamics ATTN: Research Lib 2246 P.O. Box 748 Fort Worth, TX 76101

DISTRIBUTION LIST

No. of Copies	Organization
1	General Electric Company, RESD ATTN: R. A. Larmour 3198 Chestnut Street Philadelphia, PA 19101
2	Grumman Aerospace Corporation ATTN: R. E. Melnik L. G. Kaufman Bethpage, NY 11714
2	Lockheed-Georgia Company ATTN: B. H. Little, Jr. G. A. Pounds Dept. 72074, Zone 403 86 South Cobb Drive Marietta, GA 30062
1	Lockheed Missiles and Space Company ATTN: Tech Info Center 3251 Hanover Street Palo Alto, CA 94304
4	Martin-Marietta Laboratories ATTN: S. H. Maslen S. C. Traugott K. C. Wang H. Obremski 1450 S. Rolling Road Baltimore, MD 21227
2	McDonnell Douglas Astronautics Corporation ATTN: J. Xerikos H. Tang 5301 Bolsa Avenue Huntington Beach, CA 92647
1	McDonnell-Douglas Corporation Douglas Aircraft Company ATTN: T. Cebeci 3855 Lakewood Boulevard Long Beach, CA 90801

No. of Copies	Organization
2	Sandia Laboratories ATTN: F. G. Blottner Tech Lib Albuquerque, NM 87115
2	United Aircraft Corporation Research Laboratories ATTN: M. J. Werle Library East Hartford, CT 06108
1	Vought Systems Division LTV Aerospace Corporation ATTN: J. M. Cooksey Chief, Gas Dynamics Lab, 2-53700 P.O. Box 5907 Dallas, TX 75222
1	Arizona State University Department of Mechanical and Energy Systems Engineering ATTN: G. P. Neitzel Tempe, AZ 85281
3	California Institute of Technology ATTN: Tech Library H. B. Keller Mathematics Dept. D. Coles Aeronautics Dept. Pasadena, CA 91109
1	Cornell University Graduate School of Aero Engr ATTN: Library Ithaca, NY 14850
2	Illinois Institute of Tech ATTN: M. V. Morkovin H. M. Nagib 3300 South Federal Chicago, IL 60616

DISTRIBUTION LIST

No. of Copies	Organization
1	The Johns Hopkins University ATTN: S. Corrsin Dept of Mechanics and Materials Science Baltimore, MD 21218
3	Massachusetts Inst of Tech ATTN: E. Covert H. Greenspan Tech Lib 77 Massachusetts Avenue Cambridge, MA 02139
2	North Carolina State Univ Mechanical and Aerospace Engineering Department ATTN: F. F. DeJarnette J. C. Williams Raleigh, NC 27607
1	Notre Dame University ATTN: T. J. Mueller Dept of Aero Engr South Bend, IN 46556
2	Ohio State University Dept of Aeronautical and Astronautical Engineering ATTN: S. L. Petrie O. R. Burggraf Columbus, OH 43210
2	Polytechnic Institute of New York ATTN: G. Moretti S. G. Rubin Route 110 Farmingdale, NY 11735
3	Princeton University James Forrestal Research Ctr Gas Dynamics Laboratory ATTN: S. M. Bogdonoff S. I. Cheng Tech Library Princeton, NJ 08540
1	Purdue University Thermal Science & Prop Center ATTN: Tech Library W. Lafayette, IN 47907
1	Rensselaer Polytechnic Institute Department of Math. Sciences ATTN: R. C. DiPrima Troy, NY 12181
1	Rutgers University Department of Mechanical, Industrial and Aerospace Engineering ATTN: R. H. Page New Brunswick, NJ 08903
1	Southern Methodist University Department of Civil and Mechanical Engineering ATTN: R. L. Simpson Dallas, TX 75275
1	Southwest Research Institute Applied Mechanics Reviews 8500 Culebra Road San Antonio, TX 78228
1	University of California- Berkeley Department of Aerospace Engineering ATTN: M. Holt Berkeley, CA 94720
1	University of California- Davis ATTN: H. A. Dwyer Davis, CA 95616

DISTRIBUTION LIST

No. of Copies	Organization
2	University of California-San Diego Department of Aerospace Engineering and Mechanical Engineering Sciences ATTN: P. Libby Tech Library La Jolla, CA 92037
1	University of Cincinnati Department of Aerospace Engineering ATTN: R. T. Davis Cincinnati, OH 45221
1	University of Colorado Department of Astro-Geophysics ATTN: E. R. Benton Boulder, CO 80302
1	University of Hawaii Department of Ocean Engineering ATTN: G. Venezian Honolulu, HI 96822
2	University of Maryland ATTN: W. Melnik J. D. Anderson College Park, MD 20740
2	University of Michigan Department of Aeronautical Engineering ATTN: W. W. Wilmarth Tech Library East Engineering Building Ann Arbor, MI 48104
1	University of Santa Clara Department of Physics ATTN: R. Greeley Santa Clara, CA 95053

No. of Copies	Organization
3	University of Southern California Department of Aerospace Engineering ATTN: T. Maxworthy P. Weidman L. G. Redekopp Los Angeles, CA 90007
1	University of Texas Department of Aerospace Engineering ATTN: J. C. Westkaemper Austin, TX 78712
1	University of Virginia Department of Aerospace Engineering and Engineering Physics ATTN: I. D. Jacobson Charlottesville, VA 22904
1	University of Washington Department of Mechanical Engineering ATTN: Tech Library Seattle, WA 98195
1	University of Wyoming ATTN: D. L. Boyer University Station Laramie, WY 82071
1	Virginia Polytechnic Institute and State University Department of Aerospace Engineering ATTN: G. R. Inger Blacksburg, VA 24061
1	Woods Hole Oceanographic Institute ATTN: J. A. Whitehead Woods Hold, MA 02543

DISTRIBUTION LIST

Aberdeen Proving Ground

Dir, USAMSAA
ATTN: DRXSY-D
DRXSY-MP, H. Cohen

Cdr, USATECOM
ATTN: DRSTE-TO-F

Cdr/Dir, USA CSL
ATTN: Munitions Div, Bldg. E3330
E. A. Jeffers
W. C. Dee
W. J. Pribyl

Dir, Wpns Sys Concepts Team
Bldg. E3516, EA
ATTN: DRDAR-ACW
M. Miller
A. Flatau

USER EVALUATION OF REPORT

Please take a few minutes to answer the questions below; tear out this sheet and return it to Director, US Army Ballistic Research Laboratory, ARRADCOM, ATTN: DRDAR-TSB, Aberdeen Proving Ground, Maryland 21005. Your comments will provide us with information for improving future reports.

1. BRL Report Number ________________________________

2. Does this report satisfy a need? (Comment on purpose, related project, or other area of interest for which report will be used.)

____

____

____

3. How, specifically, is the report being used? (Information source, design data or procedure, management procedure, source of ideas, etc.) ________________________________

____

____

4. Has the information in this report led to any quantitative savings as far as man-hours/contract dollars saved, operating costs avoided, efficiencies achieved, etc.? If so, please elaborate.

____

____

5. General Comments (Indicate what you think should be changed to make this report and future reports of this type more responsive to your needs, more usable, improve readability, etc.) ____________

____

____

____

6. If you would like to be contacted by the personnel who prepared this report to raise specific questions or discuss the topic, please fill in the following information.

Name: ________________________________

Telephone Number: ________________________________

Organization Address: ________________________________

____

____